Supporting information

In situ generation of electron acceptor to amplify the photoelectrochemical signal from Poly(dopamine)-sensitized TiO_2 signal crystal for immunoassay

Yilin Li,[a] Hong Dai,[a*] Qingrong Zhang,[a] Shupei Zhang,[a] Sihong Chen,[a] Zhensheng Hong,[b*] Yanyu Lin[c]

a College of Chemistry and Chemical Engineering, Fujian Normal University, Fuzhou 350108, P. R. China

b Fujian Provincial Key Laboratory of Quantum Manipulation and New Energy Materials, College of Physics and Energy, Fujian Normal University, Fuzhou 350108, P. R. China

c Ministry of Education Key Laboratory of Analysis and Detection for Food Safety, and Department of Chemistry, Fuzhou University, Fuzhou 350002, P. R. China

Apparatus

*Corresponding author: Fax: (+86)-591-22866135; E-mail: dhong@fjnu.edu.cn (H. Dai); winter0514@163.com (Z. H)

The PEC measurements containing Linear sweep voltammetry (LSV), Amperometric i-t curve, Electrochemical impedance spectroscopy (EIS) and incident photon-to-current conversion efficiencies (IPCE) were performed on a CHI 660 electrochemical workstation (Shanghai Chenhua Instrument Co., China) with a homemade system by utilizing a three-electrode system. Ag/AgCl electrode (sat. KCl), platinum wire, and a modified glassy carbon electrode (Φ=3 mm) were utilized as the reference, counter, and working electrode, respectively. Scanning electron microscopy (SEM, S4800 instrument), transmission electron microscopy (TEM, FEI F20 S-TWIN instrument and high-resolution TEM (HRTEM) analysis were performed on a JEOL-2100 transmission electron microscope that were applied for the structural characterization of the products.

Synthesis of TSC

The TSC was synthesized under solvothermal (HAc) and hydrothermal conditions, respectively, utilizing titanate nanowires as precursors. Synthesis of titanate nanowires was similar to the previous work [1]. Typically, 2 g of TiO_2 (anatase) was dispersed in a 100 mL of 30 M aqueous KOH solution. After stirring for 30 min, the resulting suspension was washed by diluted HAc solution until pH = 3.5. The final product was collected by centrifugation and dried at 60 °C for 12 h in air. Dispersing 200 mg of precursor titanate nanowires in 35 mL HAc solution (over 99%, weight), and then transferred into a 200 mL teflon-lined stainless steel autoclave, which was heated at 200 °C for 48 h. The final product was obtained by centrifugation and washed thoroughly with ethanol and DI water, dried at 60 °C over-night, then calcined at 400 °C for 30 min to remove the residual organics.

Fabrication of GCE/OMC/TSC/PDA electrode

Before modification, the bare glassy carbon electrode (GCE, Φ=3 mm) was

polished with 0.3 and 0.05 μm alumina slurry on chamois leather to produce a smooth surface. Then it was ultrasonicated for 20 min and washed successively with anhydrous alcohol and deionized water, and dried in air. Afterwards, 3 μL, 3 mg mL^{-1} OMC suspension was dropped on the clean GCE surface, placed it under infrared lamp until solvent was evaporated and cooled down to room temperature. The modification method of TSC (3 μL, 3 mg mL^{-1}) was similar to this procedure. The successfully modified electrode of GCE/OMC/TSC was dipped into an alkaline dopamine solution for 30 min. In brief, 1.0 mL, 0.01M of Tris was dissolved in 9.0 mL, 0.01 M of dopamine solution, and then stirred at temperature (25°C) for 15 min. The color of the solution changed from light pink to dark brown, arising from the spontaneous deposition of adherent PDA.

Characteristics of the peroxidase-like activity of BMC

Primarily, the BMC and HRP were treated in different temperatures by water bath method (from 10 °C to 90 °C), and then to produce the conjugations of PSA@BMC and PSA@HRP, respectively. Following that, the modified electrodes of GCE/OMC/TSC/PDA/Ab were immersed into the mixture solution (60 μL) containing PSA@BMC and PSA standard (1×10^{-5} ng/mL). Similarly, another groups of GCE/OMC/TSC/PDA/Ab were immersed into the mixture solution (60 μL) of PSA@HRP and PSA standard (1×10^{-5} ng/mL). After the incubation of 1 h at 4 °C, the electrodes were rinsed with the PBS (pH 7.4). Finally, the electrodes of GCE/OMC/TSC/PDA/Ab/PSA@BMC and GCE/OMC/TSC/PDA/Ab/PSA@HRP were allowed for incubation at 30 °C for 15 min in the solution consisting of 1.0 mmol/L of HQ and 0.15 mmol/L of H_2O_2. After that, the electrode was rinsed with PBS (pH 7.4) and dried for PEC measurements. In this experiment, all the testing conditions were same except the treatment of temperatures.

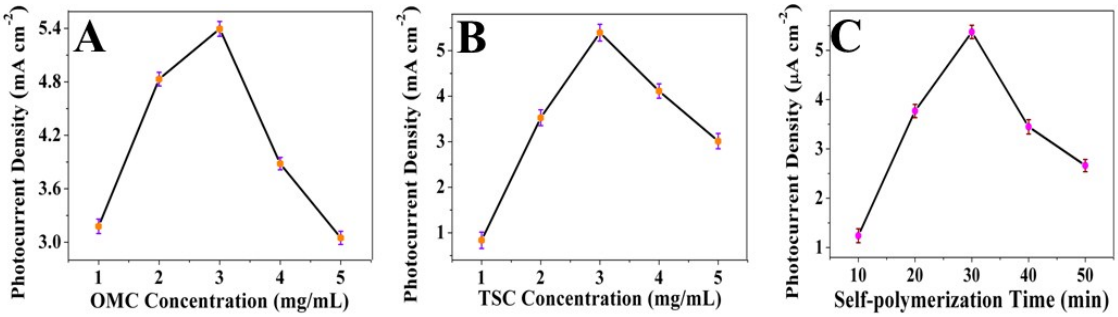

Fig. S1The optimization of this platform conditions (A) OMC concentration, (B) TSC concentration, and (C) self-polymerization time of PDA (0.01M) towards the photocurrent density of GCE/OMC/TSC/PDA in PBS (pH 7.4).

To optimize the thickness of OMC film on the surface of electrode, different concentrations of OMC suspension were prepared to construct the GCE/OMC/ TSC/PDA electrode. As exhibited in Fig. S1A, the photocurrent density gradually increased with the increasing amount of OMC from 1 to 3 mg/mL, ascribing to particular features of OMC, such as excellent electrical conductivity and large surface area, which suppressed the recombination of electron-hole pairs. Subsequently, the photocurrent descend because of the excessive OMC resulted in thicker film, causing the internal resistance and photocurrent descended. Therefore, 3 mg/mL was selected for the subsequent measurements.

The modification amounts of TSC were another important factor to affect the PEC biosensor, and the photocurrent signal of different concentrations of TSC was demonstrated in Fig. S1B. As exhibited, the photocurrent increased until 3 mg/mL TSC was dropped on the electrode surface and then decreased rapidly. It could be explained that more electrons were excited with TSC concentration increasing, causing the enhancement of the photocurrent density. However, the thicker TSC film would gather

together, impeding the transfer of the electrons and the effective light harvest, leading to the photocurrent decreased with further increasing.

To optimize the amounts of PDA, different self-polymerization times were explored to fabricate the GCE/OMC/TSC/PDA electrode. As illustrated in Fig. S1C, with the self-assembled time increasing, the more visible light was absorbed and more photo-generated electrons were driven to electrode surface due to that more PDA enhanced the stability of the PEC biosensor. Nevertheless, a deterioration of the photocurrent density was obtained with a further enhancement of the self-assembled time, attributing to the thicker PDA film would impede the transfer of the electrons from the electrode to the outside layer, leading to the photocurrent responses descended. For the sake of a significant photocurrent signal and higher sensitivity, 30 min was chosen as the optimized time for the signal recording in the following experiments.

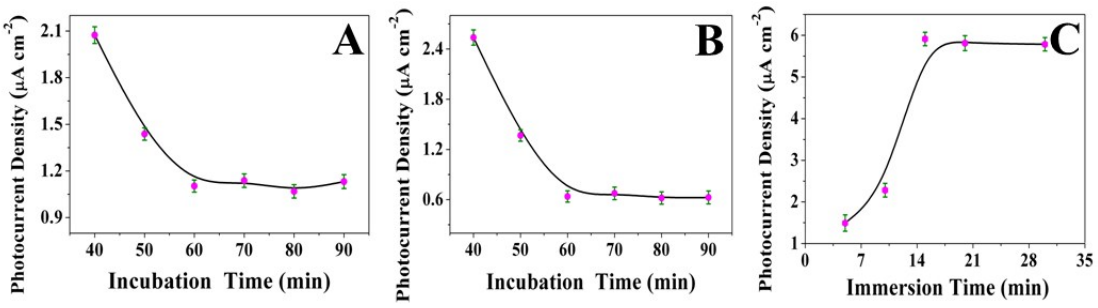

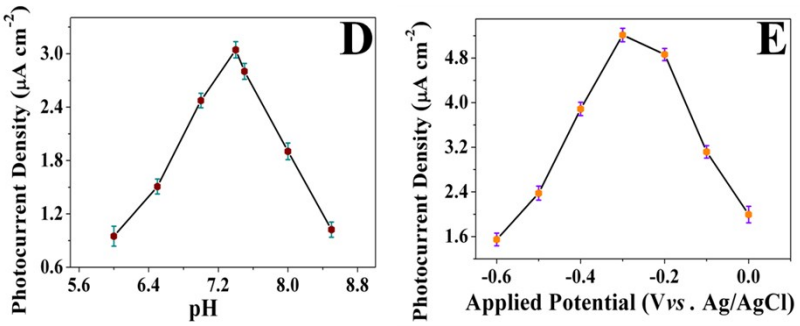

Fig. S2 The optimization of the experimental conditions of (A) anti-PSA and (B) PSA@BMC incubation time; (C) catalytic time for HQ by BMC (in the presence the H_2O_2); (D) pH value and (E) applied potential.

In the competitive assays, incubation time of anti-PSA and PSA@BMC greatly affected the sensitivity of the fabricated sensor and optimization results were shown in Fig. S2A and Fig. S2B. The photocurrent response on the PEC biosensor declined upon the increasing immersion time in 60ng/mL anti-PSA from 40 min to 60 min, and then the photoresponse remained stable. Therefore, considering the optimal analytical performance, the incubation time of 60 min was selected in the future study. Besides, the recognize time between anti-PSA and PSA also influence the sensitivity of the sensor. As demonstrated in Fig. S2B, the photocurrent density reached nearly a plateau until 60 min, indicating that abundant PSA couldn't be absorbed in the electrode. The influence of PSA@BMC catalytic time toward the PEC responses was also explored. As exhibited in the Fig. S2C, with exceeding the catalytic time, the photocurrent density enhanced, and then it reached the maximum at 15 min and maintained unchanged. In order to obtain a significant photocurrent signal and higher sensitivity, the optimum BMC catalysis time was chose 15 min for the PSA determination.

The pH value and applied potential were important factors relevant to the photo-

current response. As shown in Fig. S2D, the sensors were tested in a series of PBS with pH ranging from 6.0 ~ 8.0, the maximum photocurrent response appeared at pH of 7.4. Therefore, in order to ensure the large current density, pH 7.4 PBS was selected in following measurements. The applied potential was another key parameter that could influence the overall PEC signal, and it was also supposed to be optimized. With an increase of potential from -0.6 to -0.3 V, the photocurrent sharply improved (Fig. S2E) and the photocurrent at -0.3 V shows the maximal response for the PEC detection of PSA. The low applied potential was beneficial to the elimination of interference from other reductive species that coexisted in the real samples. Therefore, -0.3V was selected as the applied potential for the determination of PSA.

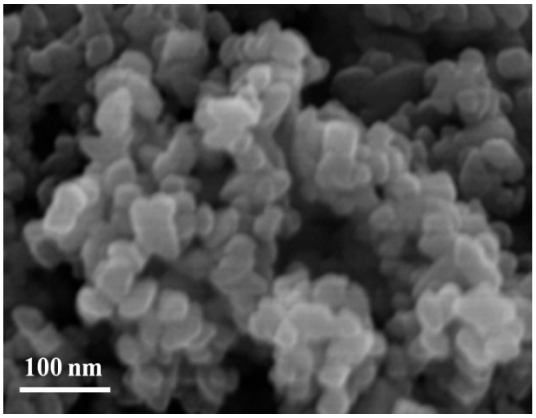

Figure S3. SEM image of TSC/PDA.

Table S1 Comparison with various methods of the PSA detection

Methods	Linear Range (ng/mL)	LOD (ng/mL)	Reference
Colorimetric immunoassay	0.005–0.5	2.9×10^{-3}	S2

Fluorescent immunoassay	0.001-20	3×10^{-4}	S3
Luminescence energy transfer	0.1172-18.75	0.1129	S4
Electrochemiluminescence (ECL)	0.005–5.0	3×10^{-3}	S5
Electrochemical (EC)	0.05-100	4.8×10^{-3}	S6
Electrochemical (EC)	0.1-100	1×10^{-3}	S7
Photoelectrochemical (PEC)	0.001-3.0	3.2×10^{-4}	S8
PEC	10^{-6}-50	3.3×10^{-7}	Present Work

Table S2 Recovery measurements of PSA in human serum samples (n=3) [a]

Sample	PSA (ng/mL)	Added PSA (ng/mL)	Measured PSA (ng/mL)	Recovery (%)
Human	0.32	0.01	0.3343	101.3

serum	0.1	0.4164	99.14
	1.0	1.41	106.8
	10.0	10.24	99.2

Reference

S1 Z. Hong, H. Dai, Z. Huang and M. Wei, *Phys. Chem. Chem. Phys.*, 2014, **16**, 7441-7447.

S2 Z. Gao, M. Xu, M. Lu, G. Chen and D. Tang, *Biosens. Bioelectron.*, 2015, **70**, 194-201.

S3 H. Pei, S. Zhu, M. Yang, R. Kong, Y. Zheng and F. Qu, *Biosens. Bioelectron.*, 2015, **74**, 909-914.

S4 J. Zhang, S. Wang, N. Gao, D. Feng, L. Wang and H. Chen, *Biosens. Bioelectron.*, 2015, **72**, 282-287.

S5 J. Li, H. Ma, D. Wu, X. Li, Y. Zhao, Y. Zhang, B. Du and Q. Wei, *Biosens. Bioelectron.*, 2015, **74**, 104-112.

S6 T. Xu, N. Liu, J. Yuan and Z. Ma, *Biosens. Bioelectron.*, 2015, **70**, 161-166.

S7 P. Jolly, V. Tamboli, R. L. Harniman, P. Estrela, C. J. Allender and J. L. Bowen, *Biosens. Bioelectron.*, 2016, **75**, 188-195.

S8 J. Zhuang, D. Tang, W. Lai, M. Xu and D. Tang, *Anal Chem*, 2015, 87, 9473-9480.